

# Identification of failure mechanisms for CFRP-confined circular concrete-filled steel tubular columns through acoustic emission signals

Dongsheng Li, Fangzhu Du, Zhi Chen and Yanlei Wang\*

*School of Civil Engineering, Dalian University of Technology, Dalian 116024, China*

*(Received May 26, 2015, Revised August 11, 2015, Accepted August 26, 2015)*

**Abstract.** The CFRP-confined circular concrete-filled steel tubular column is composed of concrete, steel, and CFRP. Its failure mechanics are complex. The most important difficulties are lack of an available method to establish a relationship between a specific damage mechanism and its acoustic emission (AE) characteristic parameter. In this study, AE technique was used to monitor the evolution of damage in CFRP-confined circular concrete-filled steel tubular columns. A fuzzy c-means method was developed to determine the relationship between the AE signal and failure mechanisms. Cluster analysis results indicate that the main AE sources include five types: matrix cracking, debonding, fiber fracture, steel buckling, and concrete crushing. This technology can not only totally separate five types of damage sources, but also make it easier to judge the damage evolution process. Furthermore, typical damage waveforms were analyzed through wavelet analysis based on the cluster results, and the damage modes were determined according to the frequency distribution of AE signals.

**Keywords:** acoustic emission; CFRP-CCFT column; clustering analysis; damage pattern recognition; health monitoring

---

## 1. Introduction

The carbon fiber-reinforced polymer-circular concrete-filled steel tubular (CFRP-CCFT) column is a new composite structure that consists of a concrete stub column that is coated with a steel layer and a CFRP layer. Several studies (Susantha *et al.* 2011, Lam and Teng 2004, Liang 2008, Eid and Paultre 2008) have indicated that both fiber-reinforced polymer (FRP)-confined concrete and steel tube confined concrete can improve structural performance significantly. Over the past three years, articles have been published on the properties of CFRP-CCFT columns (Hu *et al.* 2011, Yu *et al.* 2012, Teng *et al.* 2013). To date, however, certain damage mechanisms in this CFRP-CCFT column have not been analyzed comparatively. Moreover, the damage pattern of CFRP-CCFT columns is difficult to determine in real-time and directly through the traditional compression or bending test. To identify the damage pattern and mechanism of such columns, the acoustic emission (AE) method is proposed given its notable advantages.

---

\*Corresponding author, Associate Professor, E-mail: wangyanlei@dlut.edu.cn

AE is a real-time monitoring and non-destructive testing technique that can feasibly monitor the structural damage process. The AE system can detect released elastic waves through a transducer that is attached to the surface of the structure (Aggelis 2011, Li and Fangzhu 2016). The different AE signals for CFRP–CCFT columns are usually related to various damage sources, such as matrix cracking, fiber breakage, inter laminar debonding, and concrete crushing. Therefore, the discrimination of AE signals can help to analyze the damage mechanism of CFRP–CCFT columns. Characteristic AE features (e.g., amplitude, energy, duration, rise time, counts and frequency shown in Fig. 1) are commonly extracted to analyze the micro failure mechanisms of different material. AE waveform features such as duration and frequency generally carry information about the mode of the crack; additionally, AE amplitude recorded during loading proportional to the intensity of damage event, and the emission energy which is connected to the intensity of crack, AE counts characterize the oscillation frequency of damage signal. Therefore, every AE feature carries information about the damage modes and fracture process of monitored CFRP–CCFT columns. Li *et al.* (2015) conducted an through investigation based on the single parameter analysis to evaluate the damage severity and failure modes of CFRP–CCFT structure, recommend that the multi-parameter analysis is necessary for damage identification.

However, concerning the fact that the combination of FRP composite, steel and concrete make the failure mechanism and damage pattern of CFRP–CCFT columns more complexity. To this end, a cluster analysis is conducted on the basis of complex data types to discriminate different types of AE signals. The signals can be clustered according to their characteristics through an unsupervised pattern recognition method without introducing any advanced assumptions on the number or structure. The similarity among these signals is measured based on a parameter such as the similarity coefficient or the distance in a certain parameter space. Then, the signals are separated from one another according to a spatial criterion (Gutkin *et al.* 2011, Momon *et al.* 2012, Yang *et al.* 2015). Cluster analysis is widely conducted in various fields, such as mathematics, computer science, statistics, and engineering science. Researchers have recently applied this technique to AE signal analysis via different methods; Pashmforoush *et al.* (2011) characterized the damage to a glass/epoxy composite during a three-point bending test using the k-means and genetic algorithms. Godin *et al.* (2004) employed both supervised and unsupervised techniques for the signal clustering of unidirectional glass/polyester composites. Marec *et al.* (2008) performed principal component analysis to reduce the number of correlated variables into a small number of uncorrelated variables before clustering the principal components through the fuzzy c-means (FCM) approach.

Wavelet transform (WT) is the decomposition of a time domain signal into shifted and scaled versions of mother wavelet in different frequency band, which has been proved to be suitable for AE signal processing (Yaghoob and Mette 2015, Gang 2000, Fotouhi *et al.* 2015<sup>1</sup>). WT has good time and poor frequency resolution at high frequency band, and good frequency and poor time resolution at low frequencies, indicates that WT is an ideal approach to analyze the transient and nonlinear properties of AE signals. Considering the complication of AE signals from general composite materials, Ni and Iwamoto (2002) established the process of the WT of AE signals detected from a fragmentation test. Zitto *et al.* (2015) studied AE signals generated from dynamic tests adopted on a reinforced concrete slab with a shaking table by continuous wavelet transform (CWT). Fotouhi *et al.* (2011) conducted both wavelet transform and fuzzy c-means clustering to identify the damage properties of composite materials during three-point bending test.

In the current study, the CFRP–CCFT columns are tested via axial compression and are monitored by the AE system. Representative features such as rise time, energy, counts, duration,

and amplitude are extracted for cluster analysis by means of FCM approaches. We can then determine the damage mechanism of CFRP–CCFT columns by integrating the cluster analysis. Subsequently, the varied waveforms of AE damage are analyzed through wavelet analysis based on the cluster results.

## 2. Data processing algorithms

### 2.1 Fuzzy C-Means (FCM) algorithm

A hard cluster algorithm (k-means) crisply classifies a data point as either belonging to a cluster or not and can clusters dataset precisely<sup>[14]</sup>. Nonetheless, most clusters adhere to a fuzzy concept. FCM is a major method of unsupervised pattern recognition analysis and a data clustering technique wherein each data point belongs to a cluster to some degree; this inclusion is specified by a membership grade. This cluster analysis algorithm was first presented by Bezdek in 1981 and is advantageous over previous cluster analysis methods because it is based on fuzzy set theory. The objective of the FCM algorithms to determine the cluster centers  $C_i$  that minimize the function  $J$  Marec *et al.* (2008)

$$J(U, V) = \sum_{j=1}^n \sum_{i=1}^M [u_i(x_j)]^f d^2(x_j, C_i) \tag{1}$$

where  $U$  is the fuzzy partition matrix with  $m$  lines and  $n$  columns and  $V$  is the cluster center matrix. For example

$$U = \begin{bmatrix} u_1(x_1) & u_1(x_2) & \dots & u_1(x_n) \\ u_2(x_1) & u_2(x_2) & \dots & u_2(x_n) \\ \dots & \dots & \dots & \dots \\ u_m(x_1) & u_m(x_2) & \dots & u_m(x_n) \end{bmatrix} \tag{2}$$

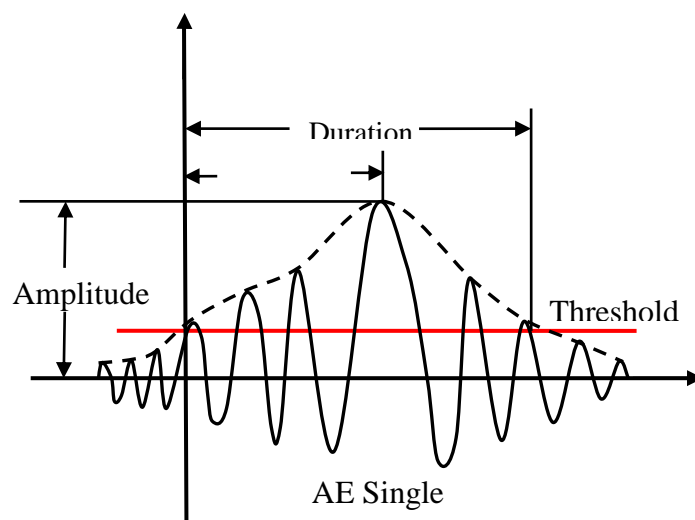


Fig. 1 Typical AE signal

$$V = [C_1 | C_2 | \dots | C_m] \quad (3)$$

where  $u_i(x_j)$  is the membership value of the  $j_{th}$  data point to the  $i_{th}$  cluster under the condition

$$\sum_{i=1}^m u_i(x_j) = 1 \quad \forall j \quad (4)$$

$d$  is the similarity matrix given in Eq. (5); this matrix characterizes similarities by utilizing the Euclidean distance measure. The elements of  $d$  are computed by

$$d_{ik} = d(x_k - v_i) = \sqrt{\sum_{j=1}^m (x_{kj} - v_{ij})^2} \quad (5)$$

The steps of the FCM algorithm can be illustrated as follows (Fotouhi *et al.* 2011, Sahu *et al.* 2012)

### 2.2 Determination of the optimal clustering number

The clustering results must be evaluated to determine whether or not reasonable. Common validity evaluation indices for cluster analysis include the partition coefficient, classification entropy, Davies–Bouldin, Hartigan, and Dunn indices (DI). In the present study, DI is applied to determine the optimal number of clusters; this index was proposed by Dunn in 1974 for compact and isolated clusters.

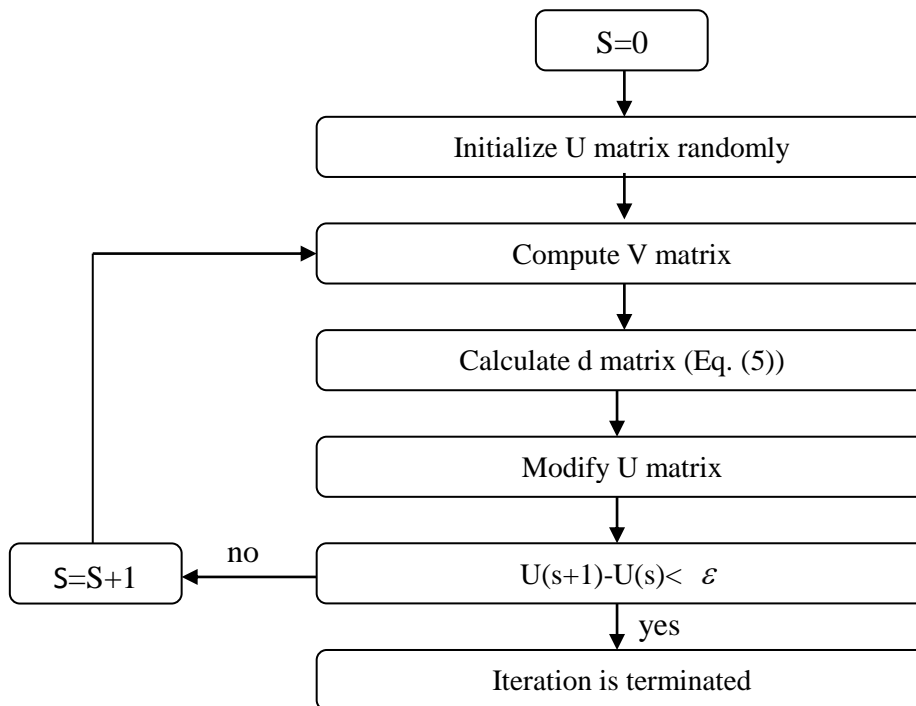


Fig. 2 Flow chart of FCM algorithm

This internal evaluation index is based on the hard clustering method, and cluster assessment relies solely on the data. DI can be calculated as follows (Sadegh *et al.* 2016)

$$DI(c) = \min_{i \in c} \left\{ \min_{j \in c, i \neq j} \left\{ \frac{\min_{x \in c_i, y \in c_j} d(x, y)}{\max_{k \in c} \left\{ \max_{x, y \in c} d(x, y) \right\}} \right\} \right\} \quad (6)$$

A large DI value indicates a compact and well-separated cluster; therefore, a maximum value corresponds to an optimal number of clusters.

### 2.3 Wavelet transform

Wavelet Transform (WT) characterizes the correlation between time signal and mother wavelet function, expressed by wavelet coefficients which can be calculated via a correlation operation between the signal  $x(t)$  and the chosen mother wavelet  $\psi(t)$ . Mathematical formulation for CWT shown in follows (Amir Mirmiran *et al.* 1999)

$$W_f(a, b) = |a|^{-1/2} \int_R x(t) \overline{\psi\left(\frac{t-b}{a}\right)} dt \quad (7)$$

Here, the mother wavelet is a localized waveform of limited duration that has an average value of zero, and drops to zero rather quickly. Scalar  $a$  and  $b$  are the scales and positions variables respectively, which is used for the shift and scale of the mother wavelet. The  $x(t)$  represent the time-domain waveform to be analyzed,  $W(a, b)$  denotes the wavelet coefficient which indicates the correlation between signal  $x(t)$  and the mother wavelet, parameter  $|a|^{-1/2}$  is applied to ensure preservation, in conjunction with Parseval’s theorem in wavelet transform.

Specially, assign that  $a = a_0^j$  and  $b = ka_0^j b_0$ , where  $j \in Z$  represent the decomposition level and  $a_0 \neq 1$  is a constant. This is the so called discrete wavelet transform (DWT).

### 3. Experimental setup

A total of six CCFT columns with two different CFRP wrapped layers were tested; three specimens of each type of CCFT column were fabricated to determine reproducibility. The column is 510 mm high, with a 170 mm diameter. Detailed manufacture process CFRP–CCFT columns shown in the previous literature<sup>[10]</sup>, the finished experimental specimen is shown in Fig. 3. Basic information regarding the two different types of CFRP–CCFT columns is shown in Table1.

All specimens are tested on an axial loading machine with 10000 kN. Two R15- $\alpha$  (50-200 kHz) resonant sensors were arranged symmetrically in the middle of each column and connected to the AE monitoring system via a preamplifier. Two displacement meters were set on the loading station to measure axial displacement, and axial compression tests were conducted with a load speed of 0.5 mm/min. The mechanical data on specimens were collected by the dynamic data acquisition system. The axial load is obtained from 5000 kN force sensors. Displacement and strain data are obtained from the displacement meter and strain gages. All AE signals are recorded by the

MISTRAS-2001 AE monitoring system, which is manufactured by the American Physics Acoustic Corporation. Detailed acquisition parameter settings for AE system were shown in Table 2. Pencil lead break tests were performed before each compression test, to verify that the system was functioning properly. As per the study conducted by Amir *et al.* (1999), the damage frequency of a FRP-confined concrete column is typically distributed between 100 kHz and 250 kHz; therefore, the band-pass filtering frequency for this study ranges from 100 kHz to 400 kHz. The test loading device and the monitoring system are depicted in Fig. 4.

Table 1 Basic Information of CFRP–CCFT Columns

Specimen type	Concrete strength	Steel tube		CFRP	
		Thickness(mm)	Radius–thickness ratio( $D_s/t_s$ )	Number of layers	Thickness (mm)
P-2-1	C60	2	87	1	0.17
P-2-2	C60	2		2	0.34

Table 2 Detailed acquisition parameter settings for AE system

Item	Threshold	Sampling rate	preamplifier gain	main gain	PDT/ $\mu$ s	HDT/ $\mu$ s	HLT/ $\mu$ s
Value	40 dB	5 MSPS	40 dB	20dB	300	800	1000



Fig. 3 The experimental specimens

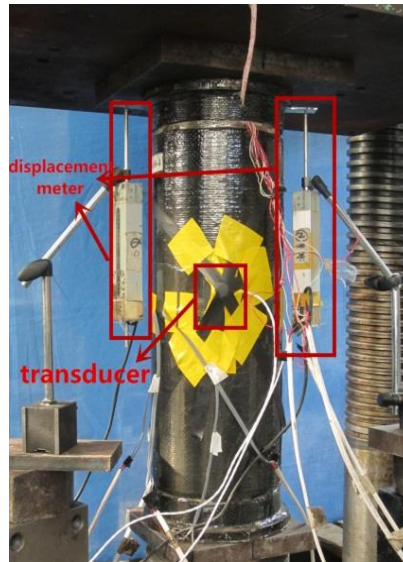


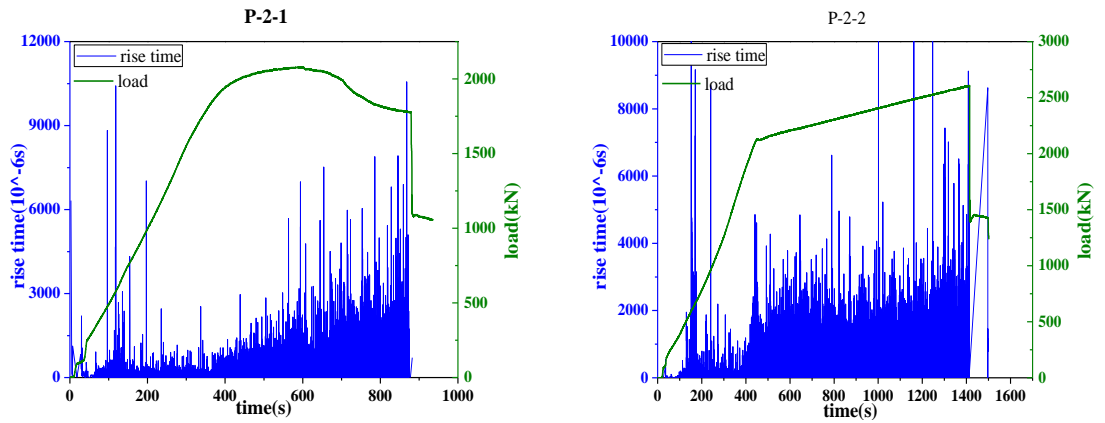
Fig. 4 Experiment loading system

## 4. Experiment results and discussion

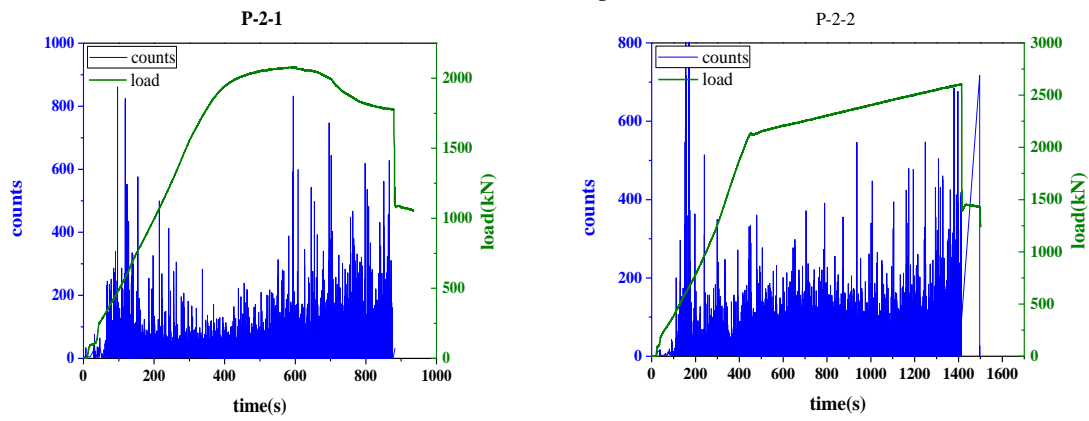
### 4.1 Analysis of the damage evolution parameters for CFRP–CCFT columns

The basic AE parameters can roughly reflect the damage condition. Matrix cracking, fiber breakage, debonding, and concrete crushing can facilitate the release of AE signals in the CFRP–CCFT columns. The risetime, counts, AE energy, and load versus time were plotted in Fig. 5; these plots can provide a rough overview of damage evolution process.

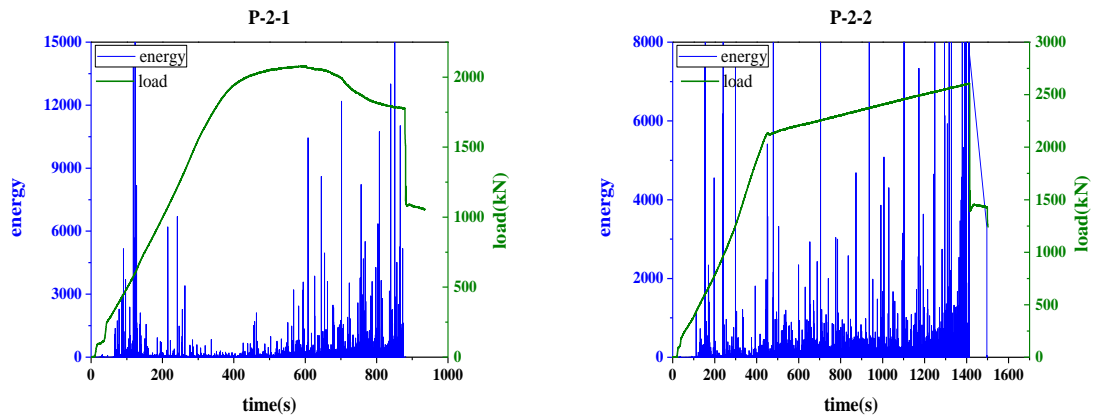
The characteristic AE features remain in low value with the exception of the initial mechanical noise at the beginning of the loading process. When the axial compressive force on the CFRP–CCFT columns reaches approximately 80% of the failure load, the values of these parameters rise sharply. This increase may be attributed to three factors, namely, concrete cracking, steel tube deformation, and CFRP fracture. Fig. 5 also indicates that the ductility of stub columns is enhanced as the number of CFRP layers increases. A column wrapped two CFRP layers exhibits clear secondary stiffness. Based on the cumulative AE characteristic parameters and the load curve that corresponds to time, the failure process of a CFRP–CCFT column can be divided into three stages, namely, the elastic, strengthening, and failure stages (Fig. 5). As the number of CFRP layers increases, the bearing capacity of the CFRP–CCFT columns improves, the strengthening stage is extended, and numerous AE signals are detected. In the event of critical failure, much AE energy is released. Pictures of the final failure condition of specimens are shown in Fig. 6. The observations of these failure profiles provided lot of damage infos, various damage modes could be observed such as concrete cracking and crushing, steel buckling and FRP fiber fracture or debonding.



(a) The rise time of specimens



(b) The counts of specimens



(c) The energy of specimens

Fig. 5 AE charactics parameter for CFRP-CCFT columns



Fig. 6 Final failure images of specimens

#### 4.2 Clustering analysis of the characteristic AE damage signals in CFRP-CCFT columns

##### 4.2.1 Determination of cluster parameters and the optimal cluster number

The result of parameter-based clustering techniques is predominantly influenced by the definition and rational selection of AE features. Many descriptors provide abundant information about AE signal characteristics, but the non-selective use of these descriptors may generate redundant information for damage mode recognition in CFRP-CCFT columns. Thus, the selected cluster parameters must not only effectively describe the feature information of AE signals, but also eliminate the interference of irrelevant factors to simplify the cluster calculation process and guarantee the speed and efficiency of the clustering algorithm. According to the AE characteristic parameter analysis introduced in section 4.1, the five temporal AE descriptors selected as the initial set for the clustering process are rise time, counts, energy, duration, and amplitude.

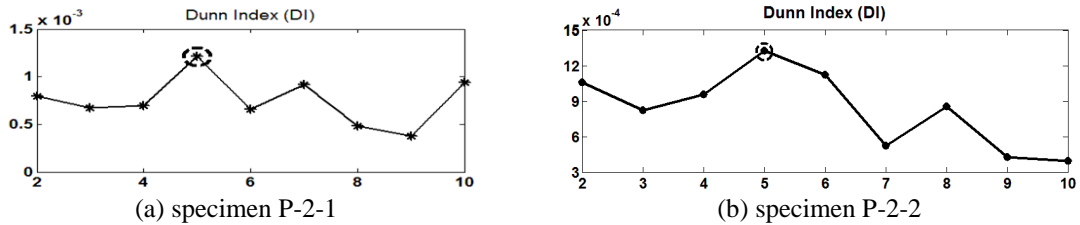


Fig. 7 Dunn Index of the CFRP-CCFT columns

DI is used to determine the optimal cluster number in the present study according to Eq. (6). Fig. 7 exhibits the DI value versus the classification number  $k$  for specimens P-2-1 and P-2-2. The value of this index is maximized when the clustering number is 5, thus indicating that the best clustering number is 5 for the AE descriptors of CFRP-CCFT columns. based on the frequency distribution of AE signals discussed later.

#### 4.2.2 Cluster analysis of the source of AE damage for CFRP-CCFT columns

In this work, the AE signals of specimens P-2-1 and P-2-2 are clustered into five categories via the FCM algorithm. The clustering results are presented in Figs. 8-11; Fig. 8 provides the count of AE signals that correspond to time after clustering, and Fig. 9 provides the cumulative signal number of each cluster type. Figs. 10 and 11 presents the AE parameter correlativity chart of amplitude-rise time, counts-duration of specimens P-2-1 and P-2-2.

According to Figs. 8 and 9 clusters D and E are mainly generated during the strengthening and failure stage of the damage evolution process for CFRP-CCFT columns, and E-type signals with minimum cumulative signal number, followed by D-type. As shown in Figs. 10 and 11, E-type signals display higher counts, longer duration, and higher energy value than cluster D-type signals, whereas the similar rise time; this outcome may be ascribed to concrete crushing, steel buckling, CFRP debonding and fracture that can be observed in Fig. 6. By comparison, cluster A, B, and C continuously distributed throughout the loading process and AE features such as counts, rise time and duration keeps in relatively lower values, whereas, cluster B and C with similar amplitude value, and type-A in maximum signals quantity with lower amplitude value and emission energy; that may be associated with the formation and development of microscopic cracks in concrete and steel tube, matrix cracking of CFRP composite, as well as with frictional sliding between steel and concrete, steel and CFRP, and the interfacial delamination of CFRP composites.

Above all, we conclude that damage types of CCFT columns coated with varied layers of CFRP composite undergoes similar failure process and damage mechanism. Considering that the complexities of damage sources in the destruction process of CFRP-CCFT columns under monotonic axial compression test, many mechanical and electromagnetic noises are inevitably generated. Different AE sources are difficult to identified precisely by cluster analysis alone; thus, representative AE waveform corresponding to each damage type is extracted and wavelet transform will be conducted to analyze the time-frequency characteristics of different damage AE signals, further classification of damage category will based on the frequency distribution of AE signals discussed later.

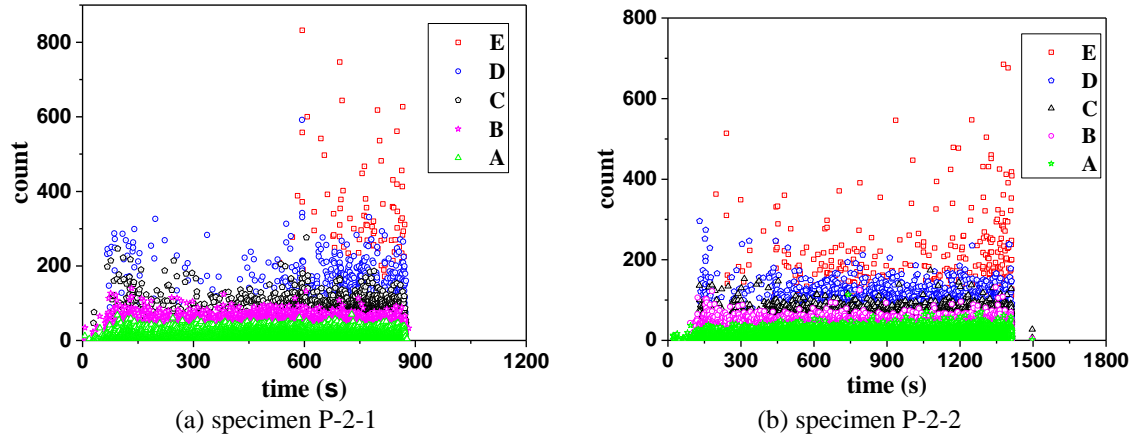


Fig. 8 The count-time chart of AE signal after cluster

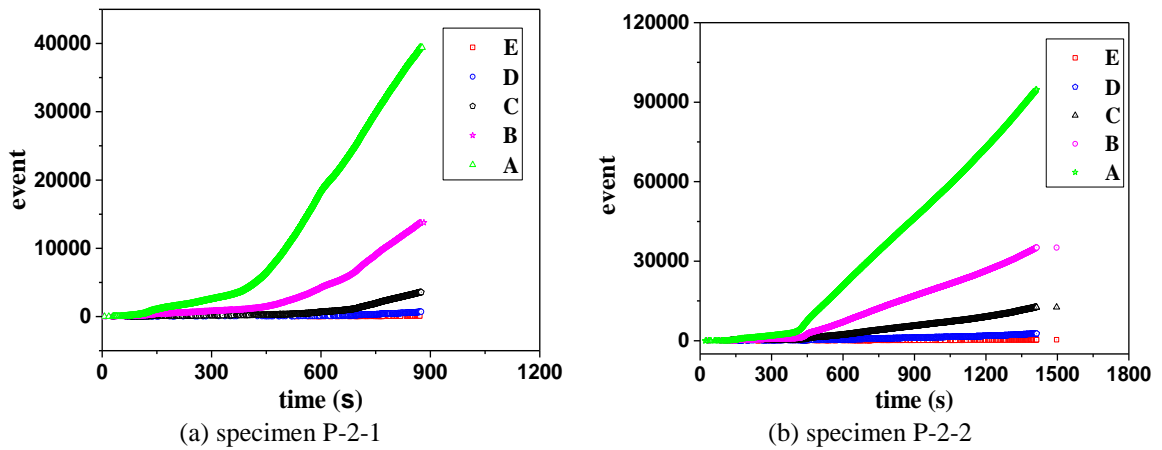


Fig. 9 The cumulative signal number of each cluster type

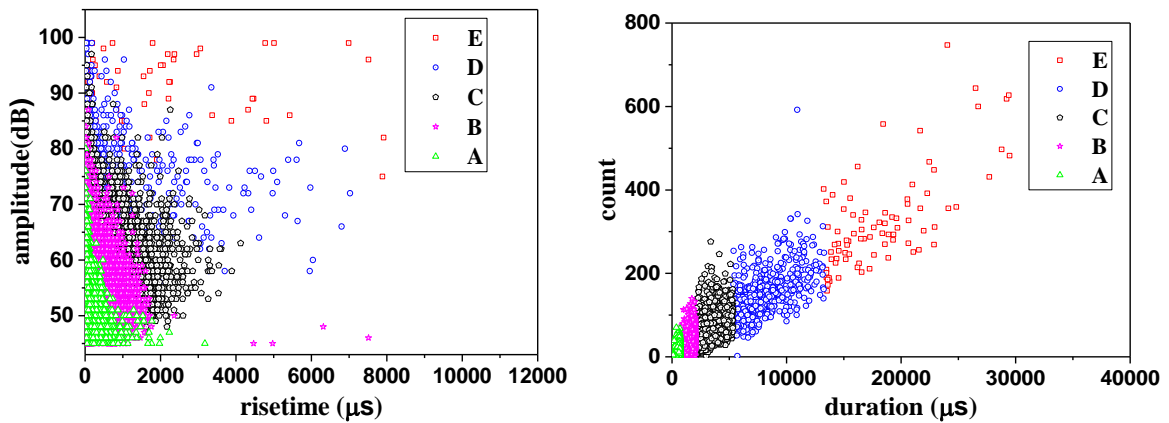


Fig. 10 The parameters correlativity chart of signal after cluster for specimen P-2-1

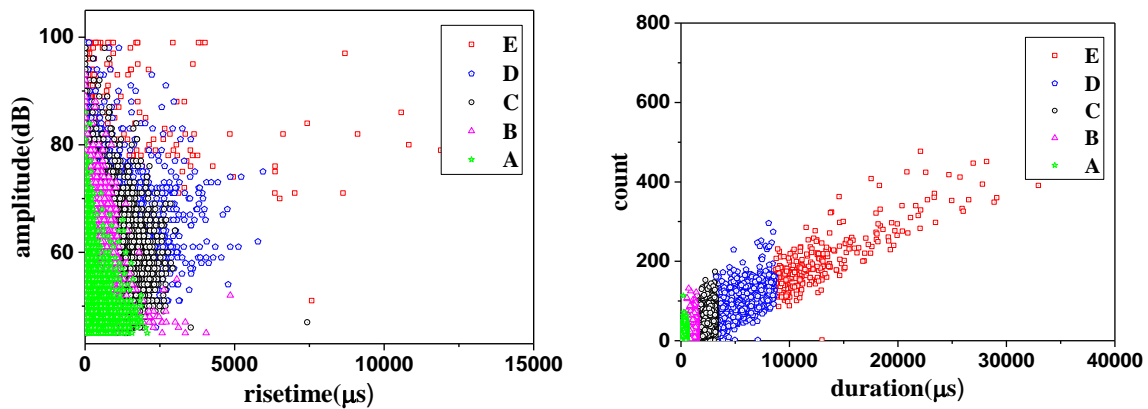


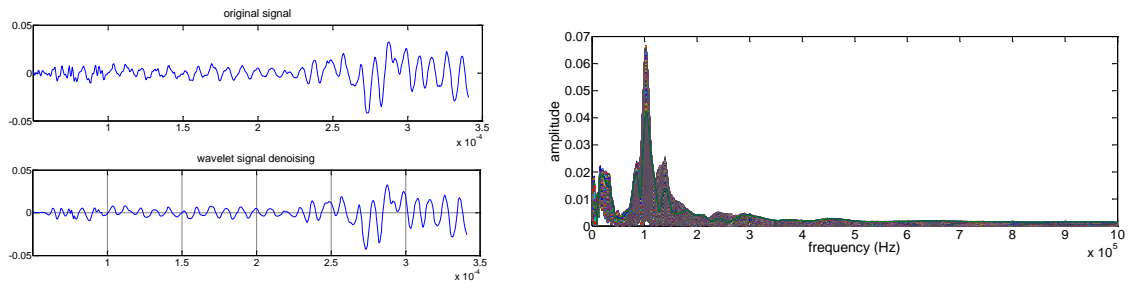
Fig. 11 The parameters correlativity chart of signal after cluster for specimen P-2-2

#### 4.3 Characteristic waveform analysis of CFRP–CCFT columns

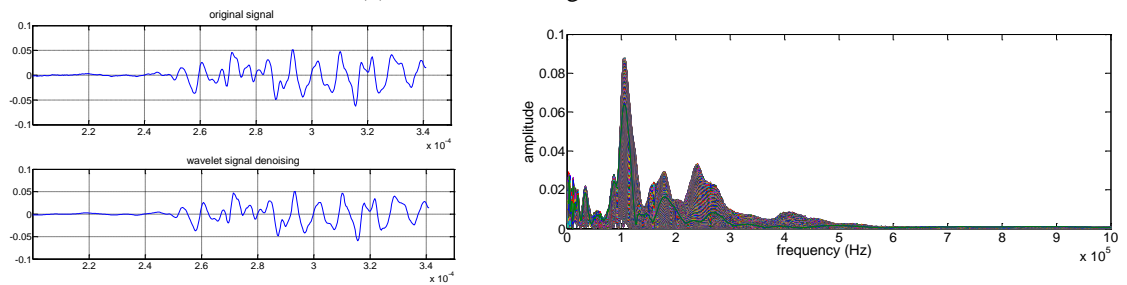
Gutkin *et al.* (2011) and De Groot *et al.* (1995) reported that the peak frequencies of CFRP fiber fractures mainly range between 300 kHz and 400 kHz, whereas the frequencies of fiber interface and peeling range between 200 kHz and 300 kHz. The common frequency of fiber matrix cracking in CFRP is approximately 100 kHz. According to the studies conducted by Yaghoob *et al.* (2015), the characteristic frequency of concrete damage mainly ranges between 100 and 400 kHz. The steel is subjected to axial tensile stress exhibits an AE frequency of roughly 100 kHz and ranges between 200 and 300 kHz; this frequency varies with the degree of damage.

Considering that specimens P-2-1 and P-2-2 have similar damage sources under monotonic compressive loading, representative AE waveforms are extracted for specimen P-2-1 in this section. All AE waveforms are de-noised through wavelet analysis prior to spectral analysis. Fig. 12 provides the signal denoising process and spectral distribution of each damage type.

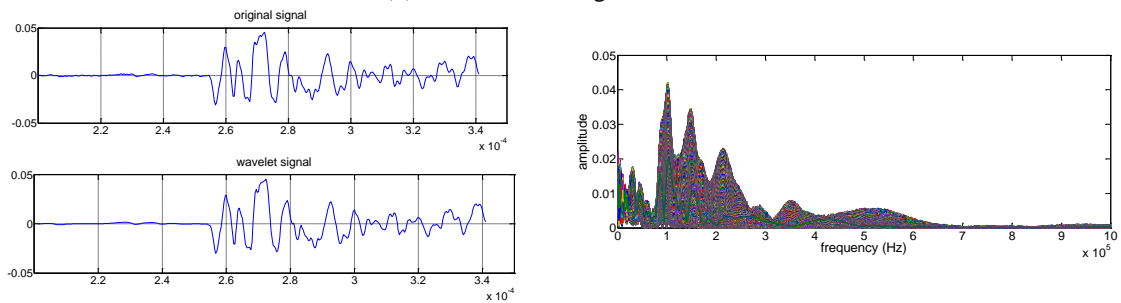
As shown in Fig. 12, AE waveform frequency of different damage types for CFRP–CCFT columns mainly concentrated at approximately 100 kHz, between 200 kHz–300 kHz and between 350 kHz–550 kHz. E-type signals with high characteristic parameter values and complex frequency components (high-frequency component with larger proportion), may be corresponding to CFRP fiber fracture and interfacial debonding, plastic deformation in steel tubes, and concrete crushing. Cluster D displays higher signal strength (higher AE amplitude and energy), AE frequency concentrate nearby 100 kHz and range of 200 kHz–300 kHz; D-type signals mainly suggest plastic deformation and buckling of steel tubes. The frequencies of cluster C range between 100 kHz–250 kHz with lower rise time and duration, mainly corresponding to the matrix cracking of CFRP composite and elastic deformation of steel tubes. For cluster B, spectral frequency mainly concentrated at roughly 100 kHz and range between 250 kHz–300 kHz; these frequencies can be associated with concrete crushing and the higher frequency component may be caused by interlaminar delamination of CFRP. Cluster A with maximum signal number, and has a single frequency of approximately 100 kHz, indicates the micro-damages of CFRP–CCFT columns such as the generating of concrete microcracks, elastic deformation of steel tubes.



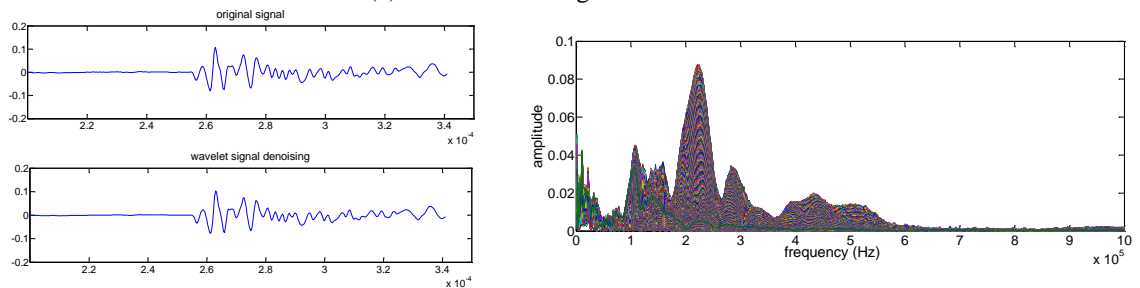
(a) Characteristic signal of cluster A



(b) Characteristic signal of cluster B

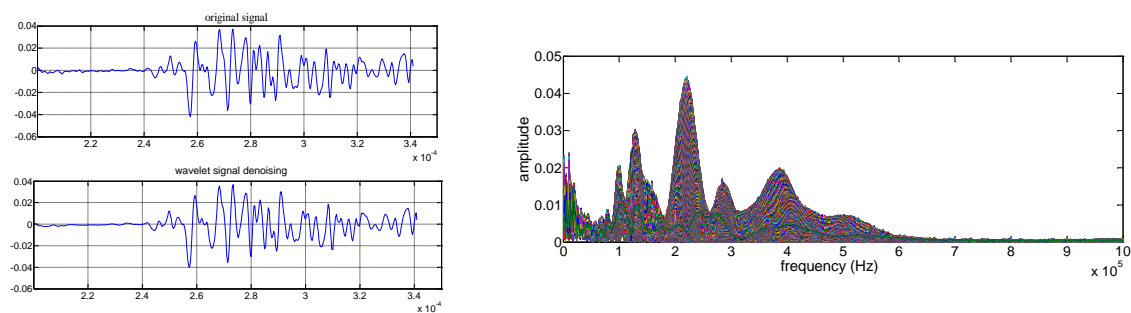


(c) Characteristic signal of cluster C



(d) Characteristic signal of cluster D

Continued-



(e) Characteristic signal of cluster E

Fig.12 Different damage characteristic signal for specimen P-2-1

In summary, combining the cluster results with wavelet spectral analysis, failure mechanisms and damage patterns of CFRP-CCFT columns under monotonic uniaxial compressive loading are effectively identified. Different damage sources are precisely characterized by representative AE feature values and primary frequency distribution. However, due to the coupling effect of various damage modes, it is really difficult to classify each observed damage pattern to a single cluster type, and the only investigation on monotonous loading condition may unconvincing, so further studies are still needed.

## 5 Conclusions

In this study, the entire destruction process of the novel proposed CFRP-CCFT columns under monotonic uniaxial compressive loading was monitored by AE technique. Damage evolution process and failure mode of CFRP-CCFT columns were studied based on the fluctuation of recorded AE signals. The clusters of AE signals from different mechanical sources were effectively obtained via the FCM algorithms. The following damage mechanisms of CFRP-CCFT columns were identified: matrix cracking, fiber fracture and debonding, steel buckling, and concrete crushing. The pattern recognition analysis was effective, and the results can be used to classify different AE signals for future monitoring. The wavelet analysis results successfully distinguish the failure types and frequency characteristics of CFRP-CCFT columns. AE waveform frequency is mainly concentrated at approximately 100 kHz and ranges between 200 and 300 kHz and between 350 and 550 kHz.

## Acknowledgements

The authors are grateful for the financial support from National Natural Science Foundation of China (NSFC) under Grant Nos. 51278083, 5147807, and the National Key Basic Research Program of China (Project No. 2012CB026200).

## References

- Aggelis, D.G. (2011), "Classification of cracking mode in concrete by acoustic emission parameters", *Mech. Res. Commun.*, **38**(3), 153-157.
- Amir M., Mohsen, S. and Hazem El, E. (1999), "Acoustic emission monitoring of hybrid FRP-concrete columns", *J. Eng. Mech. - ASCE*, **125**, 899-905.
- Degroot, P.J., Wijnen, P.A.M. and Janssen, R.B.F. (1995), "Real-time frequency determination of acoustic emission for different fracture mechanisms in carbon epoxy composites", *Compos. Sci. Technol.*, **55**(4), 405-412.
- Eid, R. and Paultre, P. (2008), "Analytical model for FRP-confined circular reinforced concrete columns", *J. Compos. Constr.*, **12**(5), 541-552.
- Fotouhi, M., Heidary, H. and Ahmadi, M. (2011), "Characterization of composite materials damage under quasi-static three-point bending test using wavelet and fuzzy C-means clustering", *J. Compos. Mater.*, **110**(46), 1795-1808.
- Fotouhi, M., Saeedifar, M. and Sadeghi S. (2015), "Investigation of the damage mechanisms for mode I delamination growth in foam core sandwich composites using acoustic emission", *Struct. Health Monit.*, **14**(3), 265-280.
- Gang, Q. (2000), "Wavelet-based Acoustic Emission characterization of composite materials", *NDT & E Int.*, **33**(3), 133-144.
- Godin, N., Huguet, S., Gaertner, R. and Salmon, L. (2004), "Clustering of acoustic emission signals collected during tensile tests on unidirectional glass/polyester composite using supervised and unsupervised classifiers", *NDT & E Int.*, **37**(4), 253-264.
- Gutkin, R., Green, C.J., Vangrattanachai, S. et al. (2011), "On acoustic emission for failure investigation in CFRP: Pattern recognition and peak frequency analyses", *Mech. Syst. Signal Pr.*, **25**(4), 1393-1407.
- Hu, Y.M., Yu, T. and Teng, J.G. (2011), "FRP-confined circular concrete-filled thin steel tubes under axial compression", *J. Compos. Constr.*, **15**(5), 850-860.
- Lam, L. and Teng, J.G. (2004), "Ultimate condition of fiber reinforced polymer-confined concrete", *J. Compos. Constr.*, **8**(6), 539-548.
- Li D.S. and Fangzhu, D. (2016), "Monitoring and evaluating the failure behavior of ice structure using the acoustic emission technique", *Cold Regions Sci. Technol.*, **129**, 51-59.
- Li, D.S., Chen, Z., Feng, Q.M. and Wang, Y.L. (2015), "Damage analysis of CFRP-confined circular concrete-filled steel tubular columns by acoustic emission techniques", *Smart Mater. Struct.*, **24** (8), 1-8.
- Liang, Q.Q. (2008), "Nonlinear analysis of short concrete-filled steel tubular beam-columns under axial load and biaxial bending", *J. Constr. Steel Res.*, **64**(3), 295-304.
- Marec, A., Thomas, J.H. and El Guerjouma, R. (2008), "Damage characterization of polymer-based composite materials: Multivariable analysis and wavelet transform for clustering acoustic emission data", *Mech. Syst. Signal Pr.*, **22**(6), 1441-1464.
- Momon, S., Godin, N., Reynaud, P., R'Mili, M. and Fantozzi, G. (2012), "Unsupervised and supervised classification of AE data collected during fatigue test on CMC at high temperature", *Compos. Part A: Appl. Sci. Manufact.*, **43**(2), 254-260.
- Ni, Q.Q. and Iwamoto, M. (2002), "Wavelet transform of acoustic emission signals in failure of model composite", *Eng. Fract. Mech.*, **69**(6), 717-728.
- Pashmforoush, F., Fotouhi, M. and Ahmadi, M. (2011), "Damage characterization of glass/epoxy composite under three-point bending test using acoustic emission technique", *J. Mater. Eng. Perform.*, **21**(7), 1380-1390.
- Sadegh, H., Mehdi, A.N. and Mehdi, A. (2016), "Classification of acoustic emission signals generated from journal bearing at different lubrication conditions based on wavelet analysis in combination with artificial neural network and genetic algorithm", *Tribology Int.*, **95**, 426-434.
- Sahu, H.B., Mahapatra, S.S. and Panigrahi, D.C. (2012), "Fuzzy C-means clustering approach for classification of Indian coal seams with respect to their spontaneous combustion susceptibility", *Fuel*

- Process. Technol.*, **104**, 115-120.
- Susantha, K.A.S., Ge, H.B.; and Usami, T. (2001), "Uniaxial stress-strain relationship of concrete confined by various shaped steel tubes", *Eng. Struct.*, **23**(10), 1331-1347.
- Teng, J.G., Hu, Y.M. and Yu, T. (2013), "Stress-strain model for concrete in FRP-confined steel tubular columns", *Eng. Struct.*, **49**, 156-167.
- Yaghoob F., Mette R.G. and Dale, B. (2015), "Acoustic emission waveform characterization of crack origin and mode in fractured and ASR damaged concrete", *Cement Concrete Compos.*, **60**, 135-145.
- Yang, L., Kang, H.S., Zhou, Y.C., Zhu, W., Cai, C.Y. and Lu, C. (2015), "Frequency as a key parameter in discriminating the failure types of thermal barrier coatings: Cluster analysis of acoustic emission signals", *Surface Coatings Technol.*, **264**, 97-104.
- Yu, T., Zhang, B., Cao, Y.B. and Teng, J.G. (2012), "Behavior of hybrid FRP-concrete-steel double-skin tubular columns subjected to cyclic axial compression", *Thin Wall. Struct.*, **61**, 196-203.
- Zitto, M.E., Piotrkowski, R., Gallego, A., Sagasta, F. and Benavent-Climent, A. (2015), "Damage assessed by wavelet scale bands and b-value in dynamical tests of a reinforced concrete slab monitored with acoustic emission", *Mech. Syst. Signal Pr.*, **60**, 75-89.